Supporting Information for

Thermodynamics of Indomethacin Adsorption to Phospholipid Membranes

Amanda D. Fearon, Grace Y. Stokes*

Department of Chemistry and Biochemistry, Santa Clara University,
500 El Camino Real, Santa Clara, CA 95053

Table of Contents **Page**

1. Chemical structures of the lipid components used in this study.

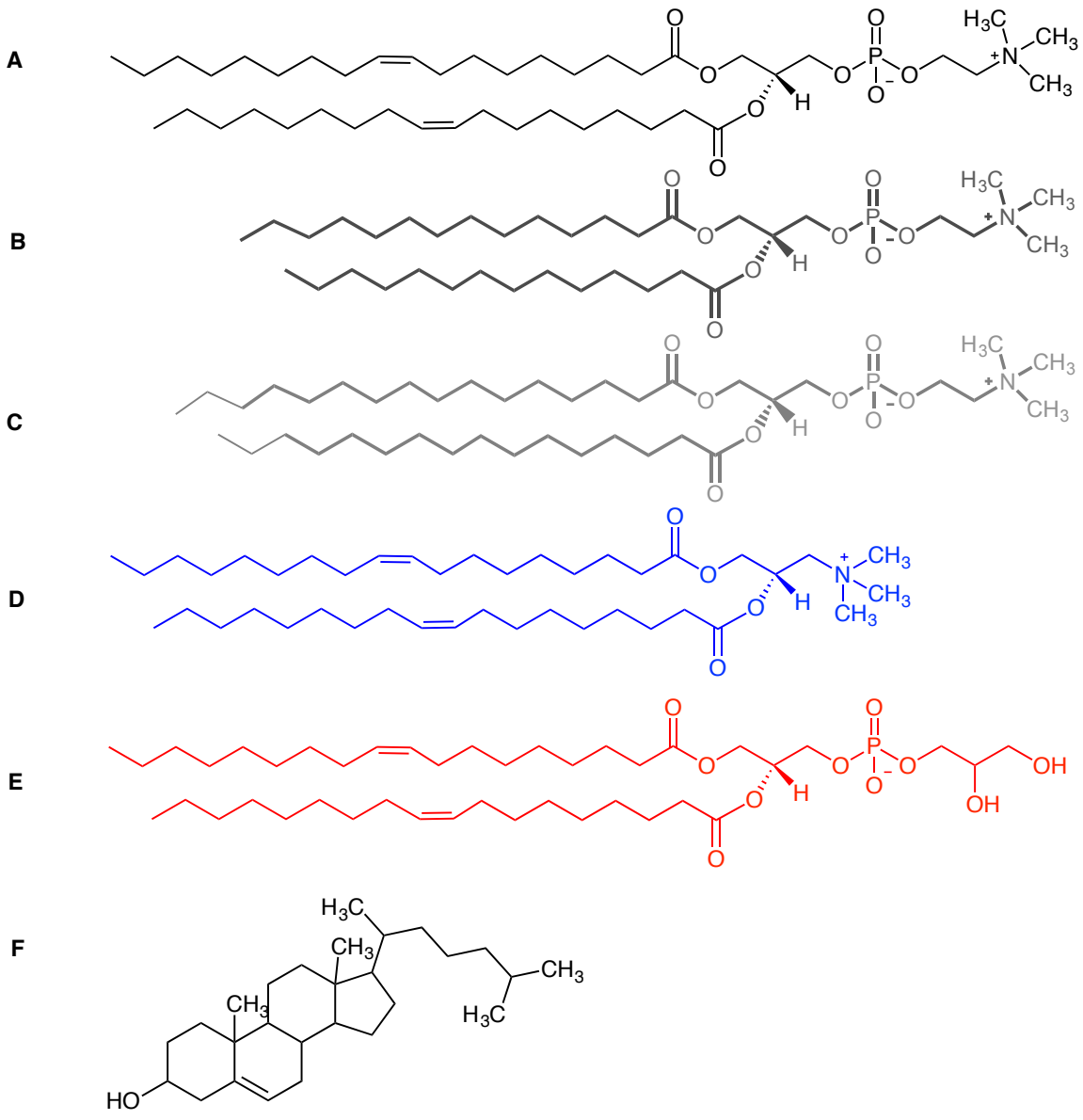

Figure S1. Chemical structures of the lipid species relevant to this study: (A) DOPC (18:1), (B) DMPC (14:0), (C) DPPC (16:0), (D) DOPG, (E) DOTAP, (F) cholesterol

2. Schematic of counter-propagating SHG setup with diagram and detailed description of flow cell.

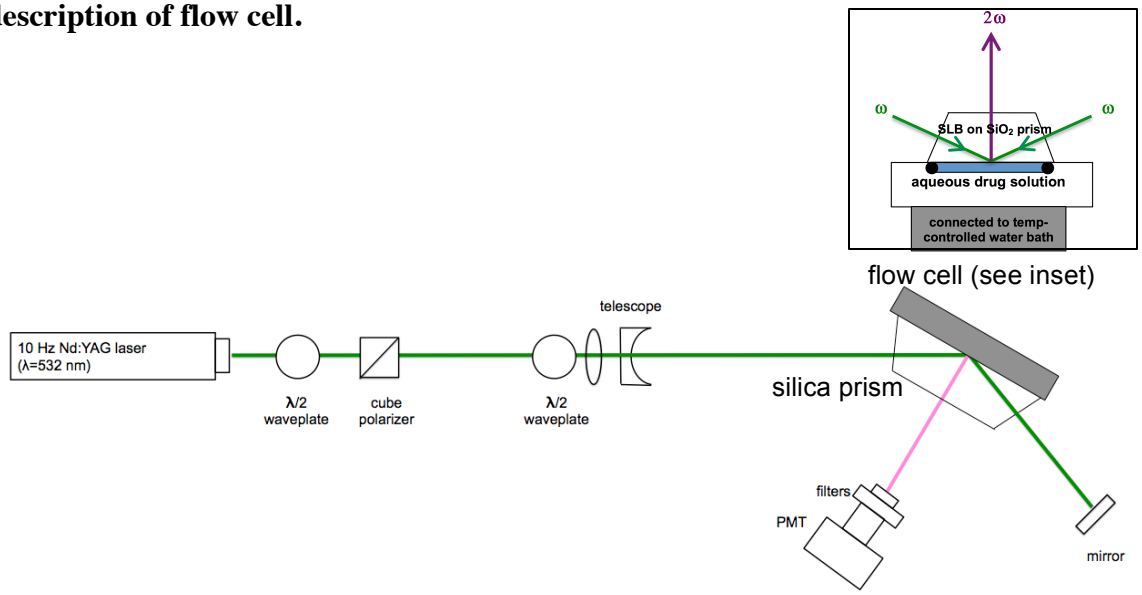

Figure S2. Schematic of counter propagating setup (and flow cell, inset).

A liquid-jacketed flow-through cell was connected to a Lauda immersion thermostat compact water bath (Type B), which allowed the aqueous drug solution to be indirectly heated. The aqueous drug solution was exposed to the main flow cell body, which was composed of the chemically resistant polymer, polychlorotrifluoroethylene (CTFE or Kel-F). A trapezoid-shaped fused silica (SiO_2) prism was purchased from Almaz Optics (material = KU-1, UV-grade SiO_2) and polished on all sides that laser light passed through or was detected through. Inlet and outlet ports utilized connectors and cap adapters made of polytetrafluoroethylene (PTFE), ferrules made of ethyltetrafluoroethylene (ETFE) and tubing made of tetrafluoroethylene (TFE). Teflon o-rings (Hydrapak, #2-015V/TE) were pressed between the SiO_2 prism and the CTFE flow cell to ensure a water-tight seal. Temperature within the flow cell was monitored continuously using a Type K thermocouples (beaded probe, VWR).

3. Polarization-dependent SHG experiments indicate orientation does not change with concentration.

indomethacin	I_{ps}	I_{s45}	Ratio of I_{ps} to I_{s45}
0	1.79 ±0.01	0.90±0.03	2.0±0.1
$1x10^{-5}$ (low)	2.10 ±0.02	1.09±0.03	1.9±0.1
$1x10^{-4}$ (high)	3.48 ±0.01	2.09±0.04	1.7±0.2

Table S1. SHG signal intensities measured at p-polarized output, s-polarized input (I_{ps}) versus SHG signal intensities at s-polarized output, 45-polarized input (I_{s45}) for indomethacin at low and high bulk concentrations.

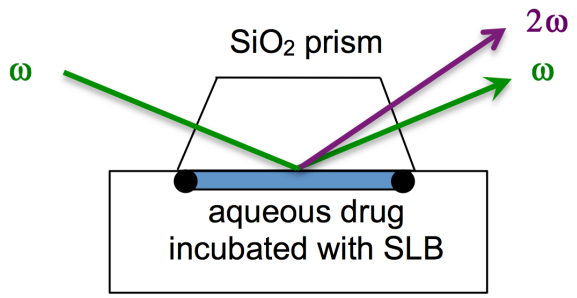

Figure S3. Schematic of co-propagating geometry used for polarization-dependent SHG experiments.

The orientation of indomethacin was monitored using polarization-dependent SHG in a co-propagating geometry. The SHG signal intensity depends on two factors—1) number of indomethacin molecules adsorbed to the lipid bilayer and 2) orientation of adsorbed drug. At high concentrations of indomethacin, the lipid bilayer may become disrupted by drug incorporation. If the adsorbed indomethacin molecules are in opposing orientations, the net dipoles of the drug molecules may cancel and result in a net cancellation of SHG signal. In this case, changes in SHG signal intensity would not accurately reflect changes in the number density of adsorbed indomethacin molecules in the lipid bilayer. To determine whether changes in orientation with increasing bulk drug concentrations contribute to changes in SHG signal intensities, we monitored polarization-resolved SHG signals using a co-propagating geometry (Figure S3). In the co-propagating geometry, two incident light waves originate from the same direction and the reflected SHG signal

generated is detected along the same optical path as the reflected incident light. The induced nonlinear surface polarization was previously derived and used to differentiate the orientation of melittin peptide[1] and breast cancer drugs[2] adsorbed to supported lipid bilayers. In the current studies, we calculated the ratios of the SHG signal intensities using s-polarized input, p-polarized output (I_{ps}) versus mixed input polarization, s-output (I_{s45}) at low and high bulk indomethacin concentrations to determine the polarization-dependent SHG response in the copropagating geometry. As shown in Table S1, the ratio of I_{ps} divided by I_{s45} are the same within the 90% confidence interval for low ($1x10^{-5}$ M) and high ($1x10^{-4}$ M) bulk indomethacin concentrations. This result suggests that changes in SHG signal intensities observed in our binding isotherms are caused by increases in the number density of adsorbed indomethacin molecules and not by changes in orientation of the adsorbed drug.

4. Derivation of simplified form of Langmuir model (Equation 4).

The nonresonant $\chi_{NR}^{(2)}$ is a real number, due to lack of electronic resonances from the lipids, water or silica at 266 nm. However, $\chi_{R}^{(2)}$ is a complex number because SHG signal is resonant with the electronic transitions of indomethacin. We can represent $\chi_{NR}^{(2)}$ as a, a real number and $\chi_{R}^{(2)}$ as b+ic, a complex number. a is the non-resonant response from the background. b and ic are the real and imaginary components, respectively, of the resonant susceptibility due to adsorbed indomethacin. We can re-write SHG intensity in eq 1 from the main text as

$$I_{SHG} \propto \left| \chi_{NR}^{(2)} + \chi_{R}^{(2)} \right|^2 \propto \left| a + N(b + ic) \right|^2 \propto (a + Nb)^2 + (Nc)^2 \qquad \text{(S1)}$$

If we assume the adsorption of indomethacin follows the Langmuir model, the surface density N in eq S1 is given by eq 2.

$$N = \frac{N_{\max} K_a [drug]}{1 + K_a [drug]} \qquad \text{(S2)}$$

In eq S2, N_{max} is the surface density at saturation, K_a is the equilibrium association constant, *[drug]* is the bulk drug concentration. Substitution of eq S2 into eq S1 results in the eq 3 and eq 4.

$$I_{SHG} \propto \left(a + b \frac{N_{\max} K_a [drug]}{1 + K_a [drug]} \right)^2 + \left(c \frac{N_{\max} K_a [drug]}{1 + K_a [drug]} \right)^2 \quad \text{(S3)}$$

$$\propto a^2 + 2ab \frac{N_{\max} K_a [drug]}{1 + K_a [drug]} + (b^2 + c^2) \left(\frac{N_{\max} K_a [drug]}{1 + K_a [drug]} \right)^2 \quad \text{(S4)}$$

The SHG intensity due to the non-resonant background in the absence of indomethacin is given by eq S5.

$$I_{SHG}^{background} \propto a^2 \qquad \text{(S5)}$$

We subtract the background contribution (eq S5) from the measured SHG signal (eq S3), we are left with eq S6.

$$I_{SHG} - I_{SHG}^{background} \propto 2ab \frac{N_{\max} K_a [drug]}{1 + K_a [drug]} + (b^2 + c^2) \left(\frac{N_{\max} K_a [drug]}{1 + K_a [drug]} \right)^2 \quad \text{(S6)}$$

To obtain SHG intensity, which changes when drug adsorbs, we use the relationship between surface density and SHG intensity from main text eqs 1 and 2, plus the relationship that states that $I_{SHG} \propto N^2$, eq 3 in the main text, to obtain eq S7.

$$I_{SHG} - I_{SHG}^{background} \propto \boxed{2\sqrt{I_{SHG}^{background}}\, b \frac{\sqrt{I_{SHG}^{\max}} K_a[drug]}{1+K_a[drug]}} + (b^2+c^2)\left(\frac{\sqrt{I_{SHG}^{\max}} K_a[drug]}{1+K_a[drug]}\right)^2 \quad \text{(S7)}$$

Note that $\sqrt{I_{SHG}^{\max}}$ is the square root of the maximum SHG intensity at surface saturation. We made the assumption that the non-resonant SHG signal intensity can be considered negligible compared to the resonant contribution and eliminated the cross-term, which is boxed in eq s7, leaving eq S8, which is the same as eq 4 in the main text.

$$I_{SHG} \propto \left(\frac{\sqrt{I_{SHG}^{\max}} K_a[drug]}{1+K_a[drug]}\right)^2 \quad \text{(S8)}$$

5. SHG data suggest that indomethacin adsorbs to SLBs in a reversible manner.

SHG signal intensities varied with polarization of the incident laser light. We recorded counter-propagating SHG polarization-dependent anisotropy curves for indomethacin adsorbed to PSLBs composed of DOPC (Figure S4a) and DMPC (Figure S4b) over 6 minutes (360 second) of exposure to the laser to ensure the origin of the achiral second harmonic emission. To evaluate reversible adsorption of indomethacin to SLBs, PBS buffer was flowed across the SLB containing adsorbed indomethacin. After injecting 40 mL of PBS buffer, the signal intensity observed from adsorbed indomethacin decreased

to the levels observed in the presence of $5x10^{-6}$ M. These data suggest that indomethacin adsorption to DOPC and DMPC lipids is fully reversible.

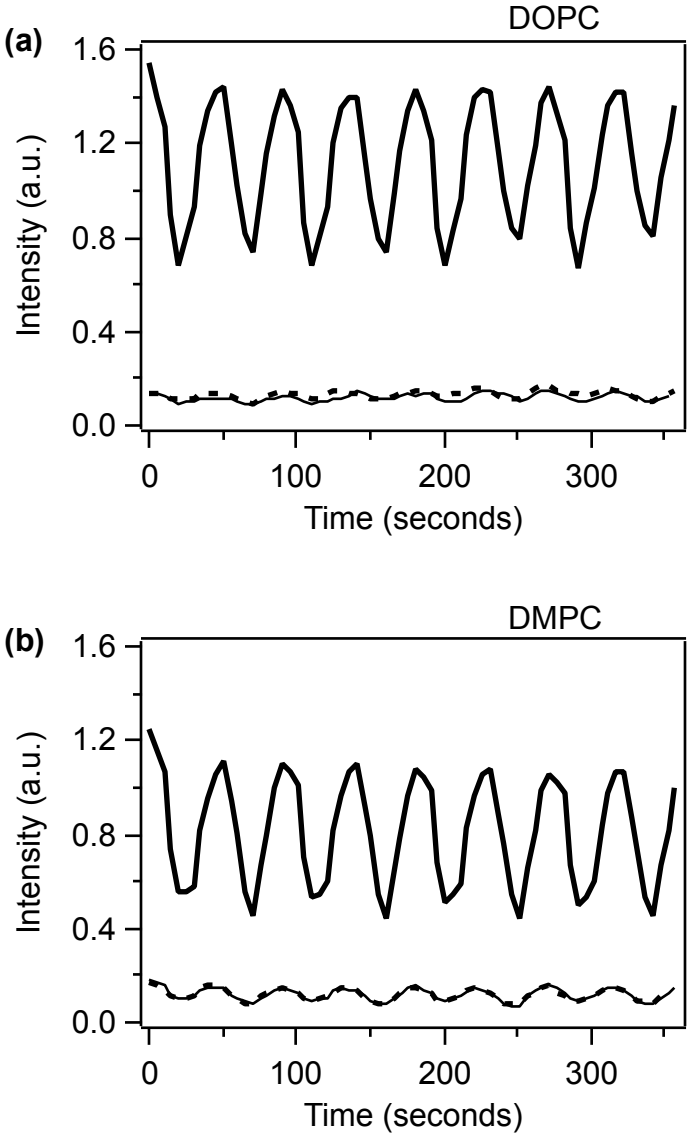

Figure S4. SHG anisotropy observed when $5x10^{-6}$ M (thin solid line) and $5x10^{-4}$ M (thick solid line) indomethacin are adsorbed to SLBs composed of DOPC (**a**) and DMPC (**b**). The dashed line is the SHG anisotropy observed after removing $5x10^{-4}$ M by injecting 40 mL PBS buffer pH 7.4.

6. Indomethacin does not adsorb to bare silica (SiO_2) in the absence of lipids.

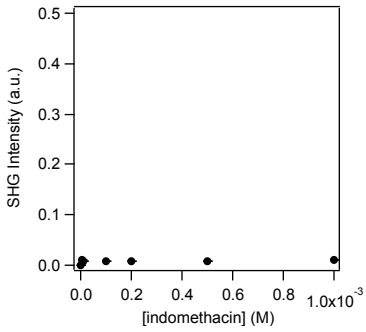

Figure S5. Negligible changes in SHG signal intensities were observed due to adsorption of indomethacin to bare silica (SiO_2) without SLBs.

7. Stability of SLBs in the presence of varying indomethacin concentrations

We collected fluorescence images of a SLB composed of 0.50% rhodamine-labeled DOPC in the presence of 0, $5x10^{-5}$, $5x10^{-4}$ and $1x10^{-3}$ M indomethacin (Figure S6). Minimal changes in the fluorescence intensities were observed after exposure to indomethacin. These fluorescence images suggest that the SLB composed of DOPC retains its structural quality during exposure to drug concentrations ranging up to $1x10^{-3}$ M. A comparison to the fluorescence intensities observed when fluorescent lipids were removed by incubation with methanol is shown in Figure S6E. These images were recorded using a 4x objective on an inverted fluorescence microscope (Olympus IX-50) equipped with a shuttered LED fluorescence excitation source (Sola SE-II). The integration time for all fluorescence measurements was 180 ms. A filter cube with an excitation filter at 540 nm (bandpass = 20 nm) and 570 nm dichroic mirror (590 nm long-pass emission filter) was used. These wavelengths overlap well with rhodamine excitation and emission wavelengths (557 nm/571 nm).

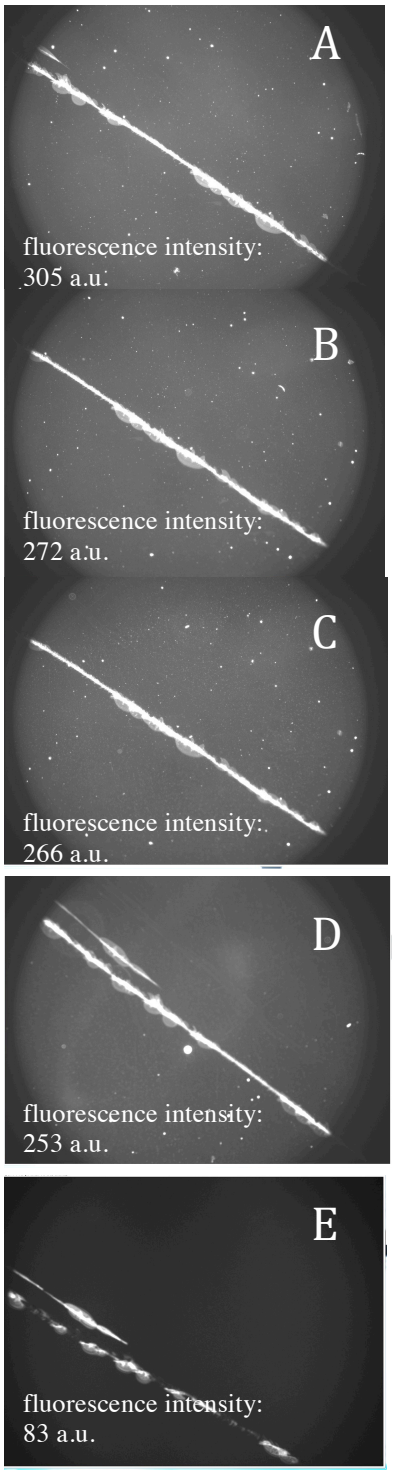

Figure S6. Fluorescence images of DOPC supported lipid bilayer containing 0.50% rhodamine-labeled DOPE in the presence of 0 M (A), $5x10^{-5}$ M (B), $5x10^{-4}$ M (C), $1x10^{-3}$ M (D) indomethacin. Comparison to fluorescence intensity when lipids were removed with methanol (E). Images were acquired with a 4x objective at 0.18 s acquisition time. A scratch was made in the glass to ensure that image was in focus.

8. Maximum surface excess and limit of detection (LOD) calculations.

To calibrate the SHG signal intensity to drug concentration in the membrane, we utilized the partition coefficient of indomethacin in a liposome-membrane system. In the linear region of the binding isotherms, at low surface densities, we expected the partitioning of the drug to the membrane to be equal to the drug concentration in a solution phase liposome.[3] By equating these two values, we calculated maximum surface excess and reported these values in Table 1. We used the experimentally-determined liposome-water partition coefficient (P_i = 1445) for indomethacin[4] and determined the membrane concentration from the aqueous concentration following eq S9.

$$[membrane] = P_i\,[aqueous] \qquad \text{(S9)}$$

Surface excess (in moles/L) is equal to the difference between the membrane and aqueous concentrations (eq S10).

$$Surface\ excess\ (moles/L) = [membrane] - [aqueous] \qquad \text{(S10)}$$

To convert from moles/L to molecules/cm^2, we take into account that a DOPC bilayer has an effective thickness of 50 Å (5×10^{-9} m) and use Avogadro's number (6.022×10^{23} molecules/mol). The sensitivity factor (*sensitivity*) used to calibrate the square root of SHG intensity ($\sqrt{I_{SHG}}$) with surface excess and was determined to be $8.2\pm2.7\times10^{-14}$ cm^2 molec^{-1} at low bulk indomethacin concentrations. Based on the calculated *sensitivity*, we used eq S11 to calculate the limit of detection (LOD) for adsorption of indomethacin to DOPC. σ is the standard deviation of the SHG signal for a blank (no drug present)

$$LOD = \frac{3\sigma}{sensitivity} \qquad \text{(S11)}$$

LOD for indomethacin was determined to be 51.6 pg/cm^2.

9. Electrostatic interactions and surface charge density correlations.

Assuming DOPC has a surface packing density of 70Å^2 for a single-component DOPC SLB or for SLBs composed of DOPC with 10% DOPG or 10% DOTAP lipids,[5] the number of charges per unit area due to incorporation of 10 mol% charged lipids is -2.29 μC/cm^2 for DOPG or +2.29 μC/cm for DOTAP. In Supporting Information Figure S7, we the square root of SHG signal intensity at saturation (sqrt I_{SHG}^{max}) was plotted versus lipid charge density and found to be linearly correlated.

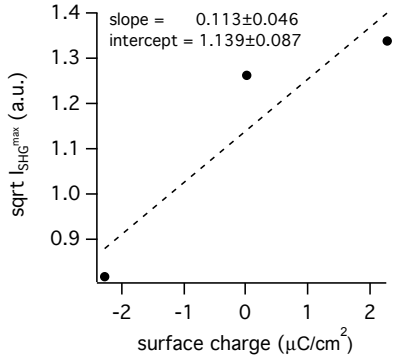

Figure S7. Linear correlation between surface charge density and surface concentration determined from square root of SHG signal intensity at saturation (sqrt I SHG max).

10. UV-Vis spectra of indomethacin in aqueous solution at varying temperatures.

As shown in Figure S7, the molar absorptivity at 266 nm increased by 1.2% (200 M^{-1} cm^{-1}) from 16700 M^{-1} cm^{-1} (at 19 °C) to 16900 M^{-1} cm^{-1} (at 45 °C). As this change in solubility is small (0.05% per °C), it does not fully account for the differences in relative

surface coverage with temperature. For example, for DOPC, relative surface coverage decreases by 0.07% per °C.

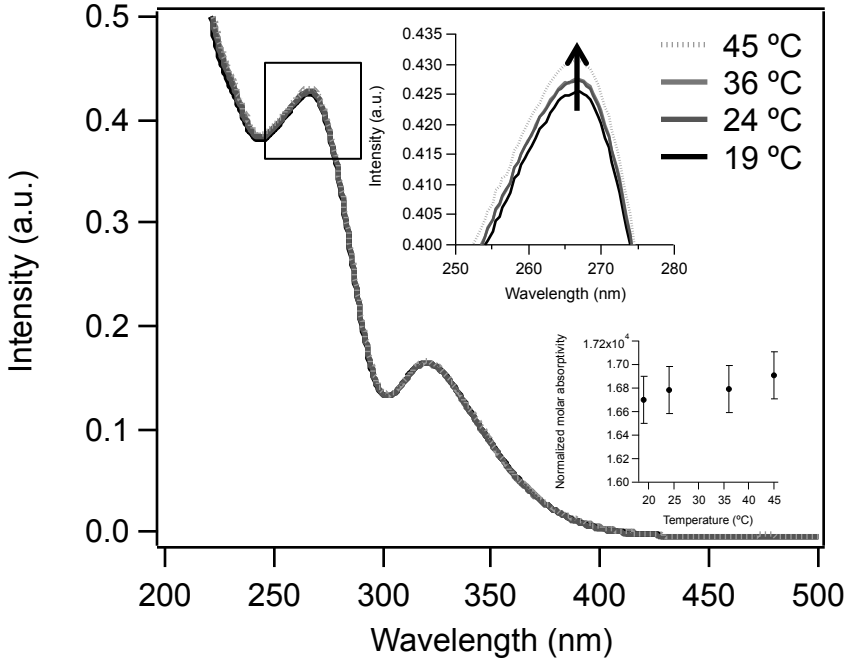

Figure S8. UV-Vis spectra of $3x10^{-5}$ M indomethacin in PBS buffer at pH 7.4 which indicate a slight increase in absorbance with temperature. Insets provide zoomed-in view of temperature data.

11. Indomethacin adsorbed to DOPC, DMPC, and DPPC at varying temperatures

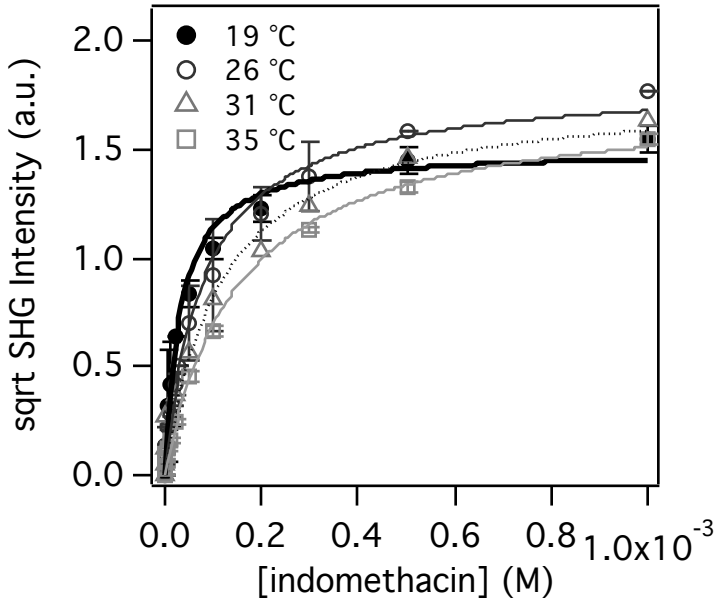

Figure S9. Adsorption of indomethacin to DOPC at varying temperatures.

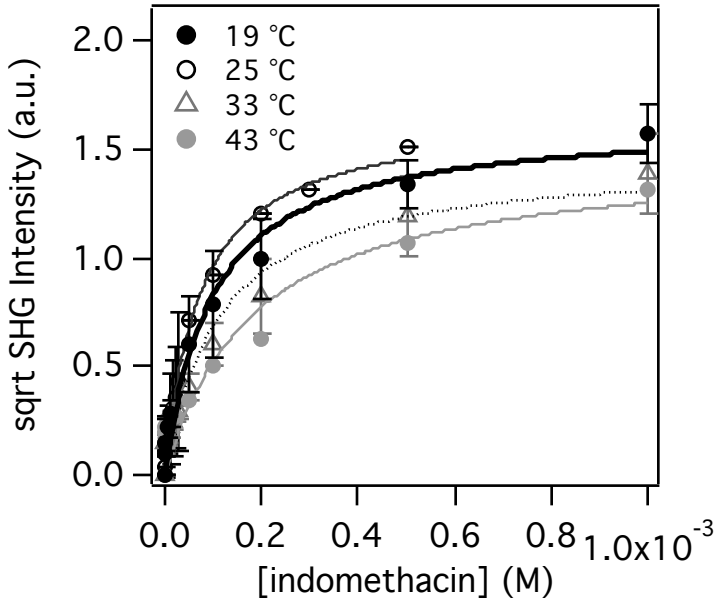

Figure S10. Adsorption of indomethacin to DMPC at varying temperatures.

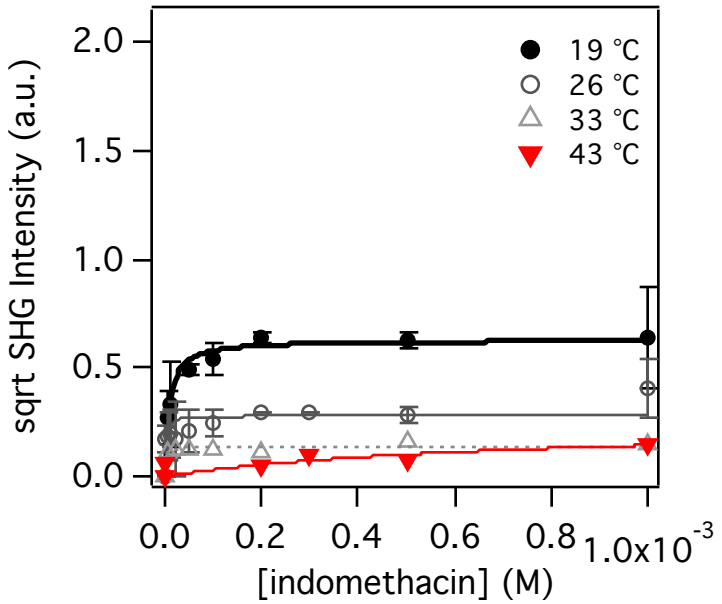

Figure S11. Adsorption of indomethacin to DPPC at varying temperatures.

For DMPC data collected at 25 °C, K_{eq} values were calculated using only with SHG adsorption data collected at aqueous indomethacin concentrations ranging from 0 to $5x10^{-4}$ M. For all other data, K_{eq} values were calculated using SHG adsorption data collected at aqueous indomethacin concentrations ranging from 0 to $1x10^{-3}$ M. DPPC data at 43 °C were not included in Van't Hoff plot.

12. Supporting Information References

(1) Kriech, M. A.; Conboy, J. C. Counterpropagating second-harmonic generation: a new technique for the investigation of molecular chirality at surfaces. *J. Opt. Soc. Am. B* **2004**, *21*, 1013-1021.
(2) Stokes, G. Y.; Conboy, J. C. Measuring Selective Estrogen Receptor Modulator (SERM)–Membrane Interactions with Second Harmonic Generation. *J. Am. Chem. Soc.* **2014**, *136*, 1409-1417.
(3) Schreier, S.; Malheiros, S. V.; de Paula, E. Surface active drugs: self-association and interaction with membranes and surfactants. Physicochemical and biological aspects. *Biochim. Biophys. Acta* **2000**, *1508*, 210-234.
(4) Esteves, F.; Moutinho, C.; Matos, C. Correlation between octanol/water and liposome/water distribution coefficients and drug absorption of a set of pharmacologically active compounds. *Journal of Liposome Research* **2013**, *23*, 83-93.
(5) Marsh, D. *Handbook of Lipid Bilayers*; Second ed.; CRC Press, 2013.